REPUBLIC OF TURKEY
AYDIN ADNAN MENDERES UNIVERSITY
GRADUATE SCHOOL OF NATURAL AND APPLIED SCIENCES
MECHANICAL ENGINEERING

EFFECT OF BORE DIMENSION AND PRESSURE ON THE CONTACT FORCES OF A SOFT BEAM

Tuncay Burcay YILDIRIM

Supervisor:
Dr. Turgay ERAY

AYDIN-2022

The thesis with the title of **"Effect of Bore Dimension and Pressure on the Contact Forces of a Soft Beam"** prepared by the Tuncay Burcay YILDIRIM, Master Student at the Mechanical Engineering Program at the Department of Mechanical Engineering was accepted by the jury members whose names and titles presented below as a result of thesis defense on 29 November 2021.

	Title, Name Surname	Institution	Signature
President :	Prof. Dr. İsmail BÖĞREKÇİ	Aydın Adnan Menderes Universiy	
Member :	Dr. Turgay ERAY	Aydın Adnan Menderes University	
Member :	Dr. Hakan ÜLKER	Bursa Technical University	

This Master Thesis accepted by the jury members is endorsed by the decision of the Institute Board Members with ……… Serial Number and ……………….. date.

Prof. Dr. Gönül AYDIN
Institute Director

ACKNOWLEDGEMENTS

Tuncay Burcay YILDIRIM

TABLE OF CONTENTS

LIST OF ABBREVIATIONS

CZM   : Cohesive Zone Modeling

FSI   : Fluid Solid Interaction

LST   : Laser Surface Texturing

PSA   : Pressure Sensitive Adhesive

PDMS   : Polydimethylsiloxane

SU-8   : SU-8 2000 is a high contrast, epoxy based photoresist designed for micromachining and other microelectronic applications.

LIST OF FIGURES

LIST OF TABLES

ÖZET

DELİK BOYUTUNUN VE BASINCININ YUMUŞAK KİRİŞİN TEMAS KUVVETLERİNE ETKİSİ

YILDIRIM T. B., Aydın Adnan Menderes Üniversitesi, Fen Bilimleri Enstitüsü, Makine Mühendisliği Anabilim Dalı, Yüksek Lisans Tezi, Aydın, 2022.

Amaç: Bu tezde, düz, pürüzsüz bir rijit gövde ile temas halindeki silindirik yumuşak kirişlerin yapışma ve sürtünme kuvvetini aktif olarak kontrol ederek, etkin eksenel, eğilme rijitliğini ve temas basıncını değiştirmek için pnömatik tabanlı bir yöntem önerilmiştir.

Materyal ve Yöntem: Bu yöntemde kirişlerin rijitliğini değiştiren yapışma ve sürtünme kuvvetinin pnömatik olarak düzenlenmesi amaçlanmaktadır.

Bulgular: Silindirik kirişlerin kiriş çapı veya yüksekliği gibi yapısal tasarım parametrelerinin ayarlanması ve böylece pasif kontrol olarak adlandırılabilecek yapışma ve sürtünme kuvvetinin değiştirilmesi üzerine çalışmalar yapılmıştır. Son zamanlarda, farklı çalıştırma mekanizmaları kullanılarak farklı yük miktarlarında yapışma ve sürtünme kuvvetinin nasıl aktif olarak değiştiğine dair çalışmalar bulunmaktadır.

Sonuç: Bu tez, yumuşak kirişlerin yapışkan ve sürtünme kuvvetinin pnömatik aktüasyon yoluyla uyarlanmasından oluşmaktadır.

Anahtar Kelimeler: Silindirik yumuşak kiriş, pasif control, yapısal tasarım parametreleri, pnömatik, hidrolik

ABSTRACT

EFFECT OF BORE DIMENSION AND PRESSURE ON THE CONTACT FORCES OF A SOFT BEAM

YILDIRIM T. B., Adnan Menderes University, Graduate School of Natural and Applied Sciences, Department of Mechanical Engineering, Master Thesis, Aydın, 2022.

Objective: In this thesis, a pneumatic-based method has been proposed to change the effective axial, bending stiffness and contact pressure by actively controlling the adhesion and friction force of cylindrical soft beams in contact with a flat, smooth rigid body.

Material and Method: In this method, it is aimed to regulate adhesive and frictional force modifying the rigidity of the beams by pneumatically.

Results: There have been studies on tuning the constructional design parameters of cylindrical beams such as diameter or height of a beam which related to changing the adhesion and friction force which can be called passive control. Recently, there have been studies on how the adhesion and friction force actively changes at different load amounts using different actuation mechanisms. (pneumatic / hydraulic, etc.).

Conclusion: This thesis consists of tailoring adhesive and friction force of soft beams via pneumatic actuation.

Key Words: Cylindrical soft beam, Constructional design parameters, Passive control, pneumatic, hydraulic

1. INTRODUCTION

In this thesis, constructional effects (bore diameter, bore height) of cylindrical beam and controlled effects (effect of pressure applied to cavity) of cylindrical beam on the adhesive and friction force will be numerically examined.

The works to be done within this thesis are explained below;

● Tuning the adhesive force by changing contact pressure between smooth surface and cylindrical beam by regulating bore pressure within beam.

● By altering the contact pressure with a pneumatic based actuation mechanism, trying to provide controllability of the adhesive force.

● The friction force of cylindrical beam in contact with a flat, smooth surface is actively controlled by regulating the effective axial and bending rigidities of the beam via pneumatic actuation.

Before examining the effect of pressurized bore, constructional parameters of the cylindrical beam must be defined and change of adhesion and friction force according to these design parameters must be obtained to model these effects on tribological response of beam. In this study, constructional and controlled parameters that affect the cylindrical beam has been examined separately. The parameters that are changed of beam dimension and bore dimension in the simulations are shown in Table 1.1

Table 1.1 Parameters that effect of the cylindrical beam

D	Outer Diameter
d	Bore Diameter
H	Height of the Beam
h	Bore Height
Ch	Height of the Wall
Th	Total Height of the Beam
P	Bore pressure

In short, numerical simulations are made for the answers of the following questions in this thesis.

- Can contact forces be controlled according to pressure and constructional parameters?

- Which is the most effective and applicable way to controlling the contact forces? Constructional or controlled parameters?

An example of the prepared simulations is shown in Figure 1.1.
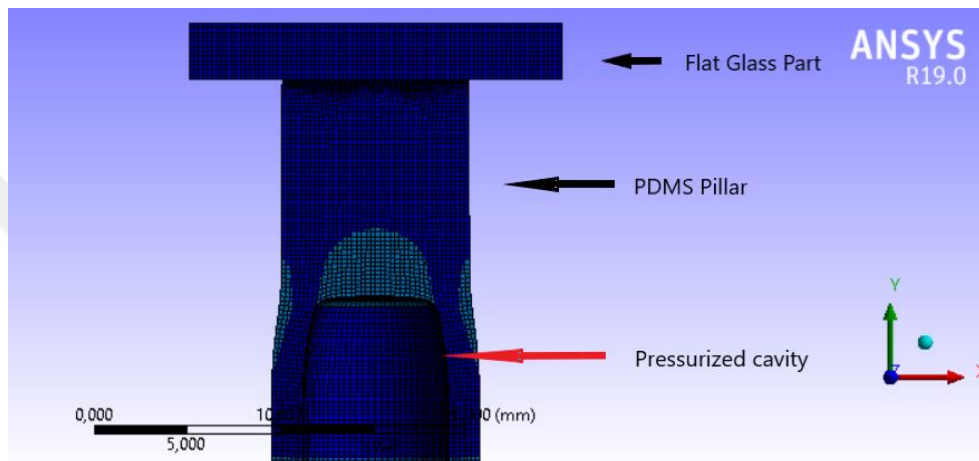
Figure 1.1 An illustration of the adhesion simulations via pressurized bore

1.1. Types of Grippers

Nowadays, mobile robots have been used frequently both in industry and in daily life and continue to be widespread. The main purpose of these robots is to make people's lives easier with their functions and to reduce the need for human workers, especially in the industry. Therefore, these robots should be able to perform human movements and repeat them in a certain cycle. One of these movements is to contact with another material and gripping. Robots with these functions are generally called as grippers.

There are many types of gripper robots according to gripping method or application area (Kumar, 2000). These gripper types are;

- Adhesive Grippers

- Mechanical Grippers

- Hooks and Scoops

- Magnetic Grippers

- Vacuum Grippers

- Expandable Blade Type Grippers

Basically, adhesive objects should be used for holding action in adhesive grippers. However, the major duty of these grippers is sticking another object, there are certain limitations of these grippers. Generally, it can be used for lightweight materials for holding, lifting and carrying actions. To carry out these actions of the grippers, it has been used adhesive materials that must have higher elasticity of modulus and high adhesive character (Kumar, 2000)

Figure 1.2 Adhesive Gripper Illustration (Kumar, 2000)

2. LITERATURE REVIEW

In the literature, it has been subject of research and development to change adhesive force of cylindrical beams, and the beams are designed so that the adhesive property of the beams gets close to adhesive characteristics of animals in nature. Gecko (Süleymancık) is the most inspired animal in the nature from the standpoint of adhesion. The underlying reason is that Geckos can adhere to any surface (rough or smooth, hydrophilic or hydrophobic), thanks to cylindrical beams that are arranged in a hierarchical way on its feet (Autumn & Gravish, 2008). Thanks to the structures on its feet, it forms a dry contact to the surface without need of any chemical reactions. In the literature, it is aimed to obtain adhesion force by forming only dry contact (Zeng et all., 2009). Usually, these artificial beams are made of polymer / elastomers by elastic characteristics. For example, Polydimethlysiloxane (PDMS) or Polyurethane. In this thesis, PDMS material is used as a soft cylindrical beam.

Although there have been previous studies on obtaining adhesive force by forming cylindrical beams, influence of friction force on adhesive force is shown experimentally (Varenberg & Gorb, 2007). For this reason, the change of friction force of cylindrical beams according to constructional and design parameters has become important (Murarash et all., 2011). This thesis aims to control of contact forces of polymer beams by tuning the rigidity of beams and pressurizing the bore dimension of beams unlike previous studies (Mari et all., 2015). In this way, the contact forces of the beam can be altered by convenient design of the beams and proper selection of pressure actuation.
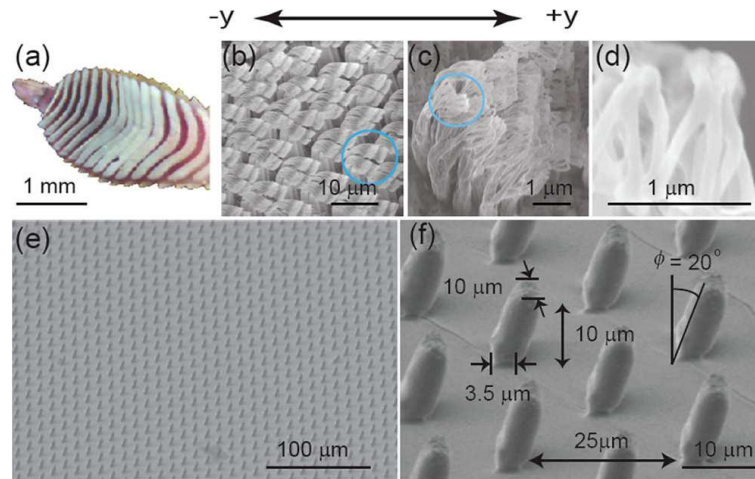
Figure 2.1 Gecko's foot nature hierarchically (a) toe, (b) seta, (c) spatula, and (d) a magnified view of a spatula pad. Scanning electron microscope (SEM) images of (e) tilted PDMS flaps and (f) enlarged view of the tilted PDMS flaps (Yu et all., 2012).

Adhesion force in the gecko adhesive and gecko imitative adhesives, the friction force F∥, which is balanced the gravity force of the body of the gecko is too important for gecko's uncommon climbing talents. Generally, adhesive friction force between two surfaces is described this equation that is shown below (Yu et all., 2012).

$$F_{\parallel} = \mu F_{\perp} + S_c A_{real}$$

At the equation above, μ represents friction coefficient, $F_{\perp}$ is the normal load, S_c is the shear strength and A_{real} is the real contact area (Gao, J. P., 2004)

2.1. Use of Polymer Cylindrical Beams: Surface Texturing

If a tribologically significant functionality is expected from two mechanical surfaces in contact with each other, it is an important option to alter one or both surfaces topographically without affecting the chemical structure between the two surfaces (Etsion, 2005). In this way, the respective surface or surfaces are provided with functionality which is called surface texturing. Surface texturing is defined as functionalization of a surface (Arslan et all., 2016). Surface texturing is carried out by adding or removing structures of similar or different geometries with one or another material on the surface of any of the two contacted surfaces. Therefore, changing constructional parameters of these structures such as height, dimension, geometry, tip geometry etc. allows us to tune tribological response of contacting surfaces (Eray et all., 2016) Figure 2.2 shows typical manufacturing of

cylindrical type of beam by using SU-8 resist and characterization of tribological response in terms of adhesive force by using an adhesion measurement device.
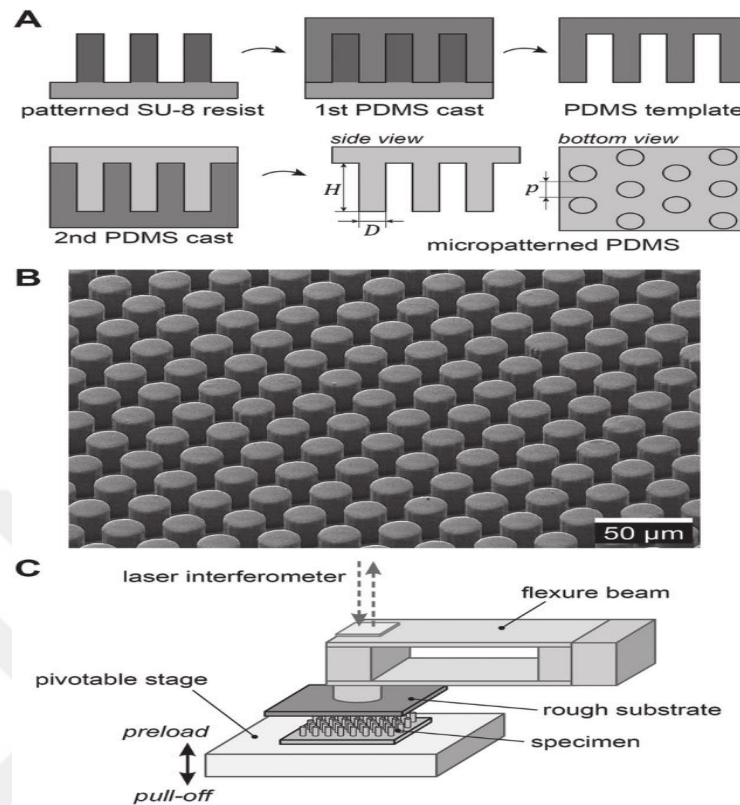
Figure 2.2 Process scheme for manufacturing micro-patterned adhesives and experimental setup for normal adhesion measurements. A) Procedure for the fabrication of polydimethylsiloxane (PDMS) pillar array specimens using pre-patterned SU-8 templates for subsequent two-step replication into PDMS. B) Scanning electron micrograph of a representative micro-patterned PDMS sample. C) Schematic illustration of the adhesion measurement device that consists of a pivotable stage for sample manipulation and a rough substrate mounted on a flexible double beam. The laser interferometer monitors the elastic deflection of the beam, from which the forces are deduced, during the measurement (Barreau et all., 2016)

2.2. Switchable Adhesion Applications

Alterable adhesion is used many applications which they are transfer printing, climbing robots, gripping tools and pick-place processes (Nasab et all,2020). Generally, elastomers are used in these devices due to high flexibility to provide adhesive contact. PDMS(Polydimethylsiloxane) is one of the common materials for high adhesive character.

There have been recent studies tuning the adhesive force via pressure. Figure 2.3 shows the simulation for adjustable adhesion force with pressurized bore cylindrical shape material.
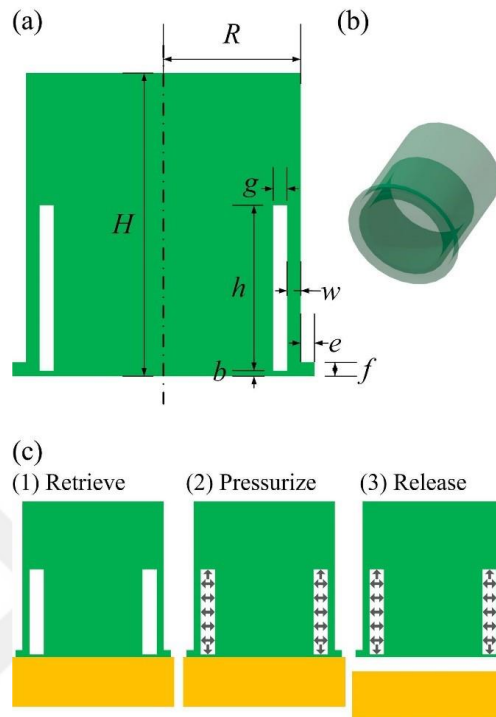
Figure 2.3 (a) 2D schematic of tunable adhesive contact via pressure (b) 3D Schematic of the device. (c) Principle of operation (Nasab et all,2020).

2.3. Control of Adhesion with Pre-Pressurized Flat Surfaces

There have been recent studies about adhesion control of pre-pressurized surfaces in the elastomers. One of these of studies indicate that, pressurizing inlet on the flat surface in PDMS material needs less adhesion force with same elongation values (Minsky, H.K., & Turner, K.T. 2015). Thus, it can be obtained more elongation with same force by help of the pressurizing inlet of the flat surfaces in the PDMS substrates. As well, adjustable adhesion force can be possible by pressure alteration. At the same time, adhesion force can be related to the constructional effects of the part.
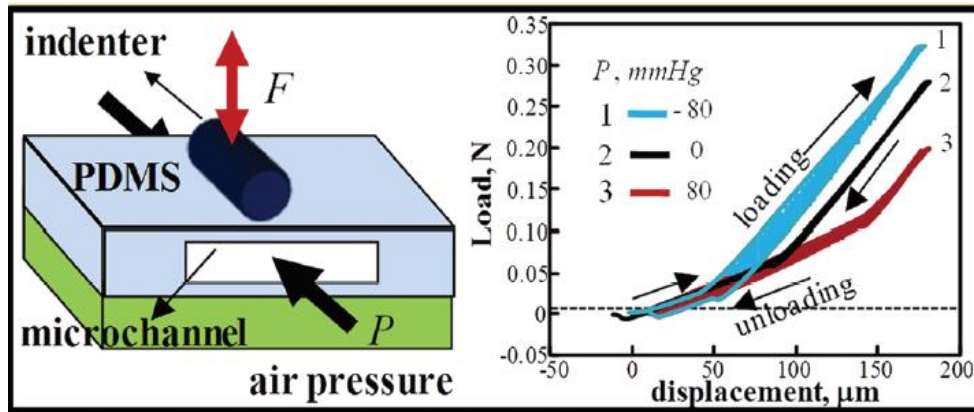
Figure 2.4 Force-displacement comparison at different pressure values in the PDMS flat surface (Minsky, H.K., & Turner, K.T. 2015)

2.4. Pressure Sensitive Adhesives (P.S.A)

Pressure sensitive adhesives (P. S.A) has been studied from number of researchers over the years, using different methods for predicting adhesive failure using peeling tests and probe tack tests. Prediction of adhesive properties in terms of constructional and controlled properties is still challenge (Verdier, C., & Ravilly, G., 2007).
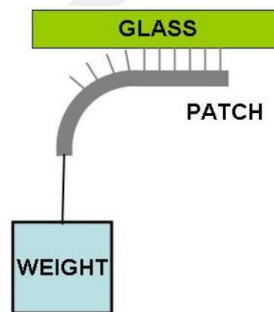
Figure 2.5 Experimental Setup of Peeling Test
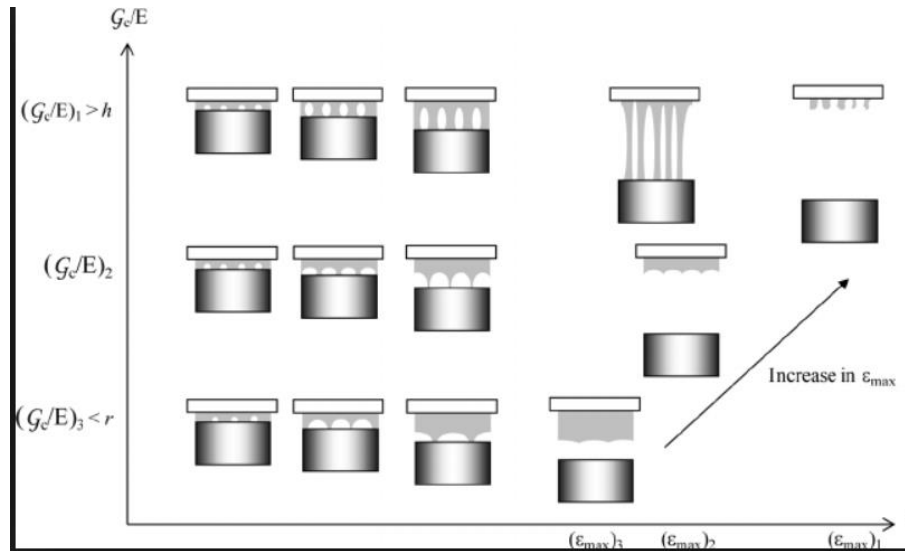
Figure 2.6 Experimental Setup of the Probe Tack Test

2.5. Adhesive Friction of PDMS

Friction and adhesion are significant factors on contact mechanics in this thesis. The effect of adhesive friction cannot be ignored. There have been different studies on adhesive friction of elastomers.

As known, elastomers have poor dry sliding friction properties due to their high adhesive character (Voyer et all., 2017).. In order to solve this problem in industrial technics, interfacing materials is used such as oils, greases, coatings. In the alternative, high adhesion characteristics of the elastomers can be reduced by modifying elastomer composition or can be enabled reducing the effective contact area such as laser surface texturing.

Laser surface texturing (LST) is the one of technique of surface texturing which is used for wide range of materials. LST has been preferred due to its superior flexibility, good accuracy of the surface texturing and better tunability (Mao et all., 2020).
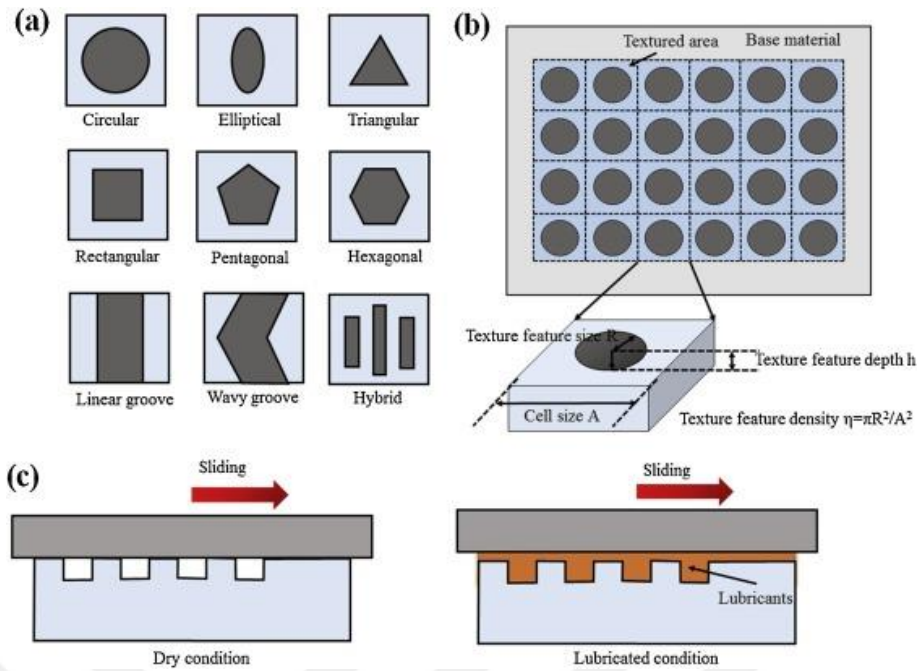
Figure 2.7 Illustration of (a) different kinds of texture feature shapes, (b) texturing parameters during LST process, and (c) the effect of texture design on the contact condition during dry and lubricated sliding (Mao et all).

2.6. Experimental setup of the adhesion measurements of PDMS material

There have been various studies about the measurement the adhesion in the PDMS specimen. One of these studies, López and Williams performed an experimental setup for switchable adhesion by using soft springs (López &Williams, 2016). Illustration figure of this experimental setup in that study is shown in Figure 2.8.
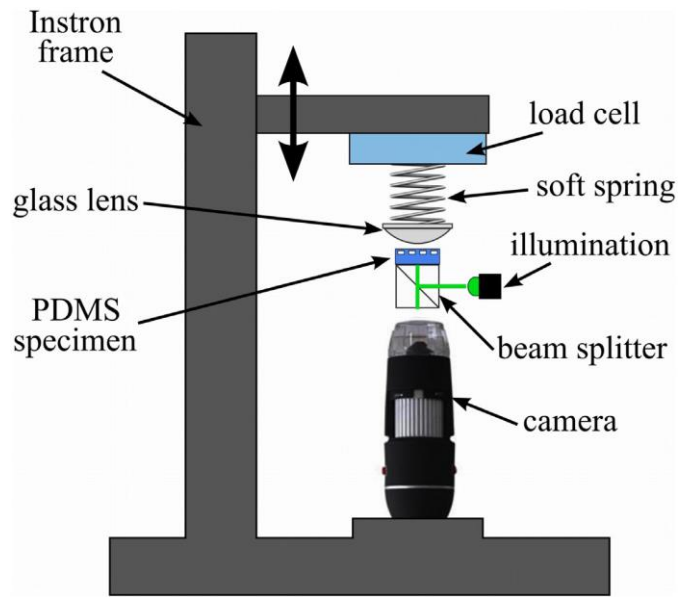
Figure 2.8 Adhesion measurements experimental setup by using soft springs (López &Williams, 2016)

In addition, pressure applying period of the experiments is important also between specimen and glass contact area. Different results are obtained by applying pressure to the part at different times. These are pre-pressurizing and pressurizing after contact that is shown in Figure 2.9.
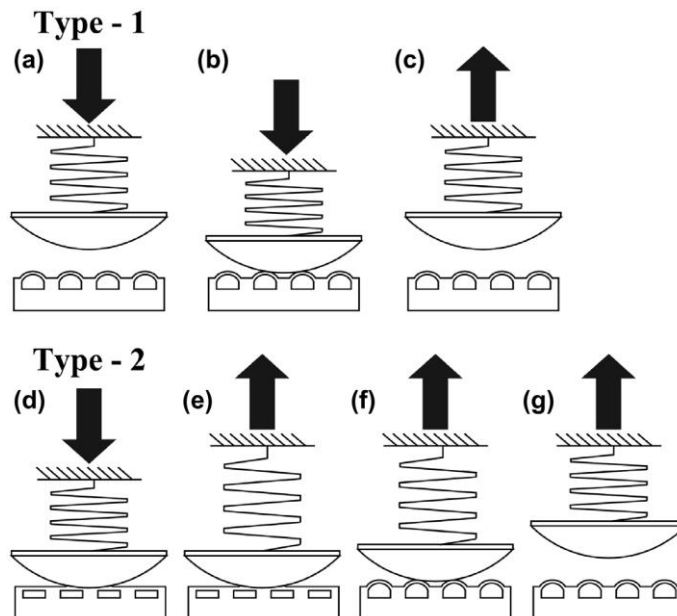
Figure 2.9 Adhesion experiments at different pressuring types ((López &Williams, 2016)

2.7. Cohesive Zone Modelling (CZM)

In this thesis, simulations have been compiled with fluent and static structural module in ANSYS finite element-based program. A fracture mechanism is necessary for separation of between bonded surfaces are like cylindrical beam and glass plane. CZM theory is used to separate the adhesive bonds between two surfaces.

CZM is used in different studies in finite element analysis. CZM concepts have been implemented for studying mode I fracture in pre-cracked bonded Double Cantilever Beam (DCB) sample. Load displacement curves are obtained from the general mechanical response from the cohesive zone parameters and these curves are compared with different CZMs. Then, it is illustrated some interesting features concerning the prediction of damage onset in adhesive joints (Alfano et all.,).

CZM is efficient method for adhesive bonded contacts in structure-level simulations. CZM provides a simplicity in computation compared to using solid elements. It also provides a more accurate representation of adhesive response, damage and failure compared to tiebreak contact processes (Hartlen et all, 2020).
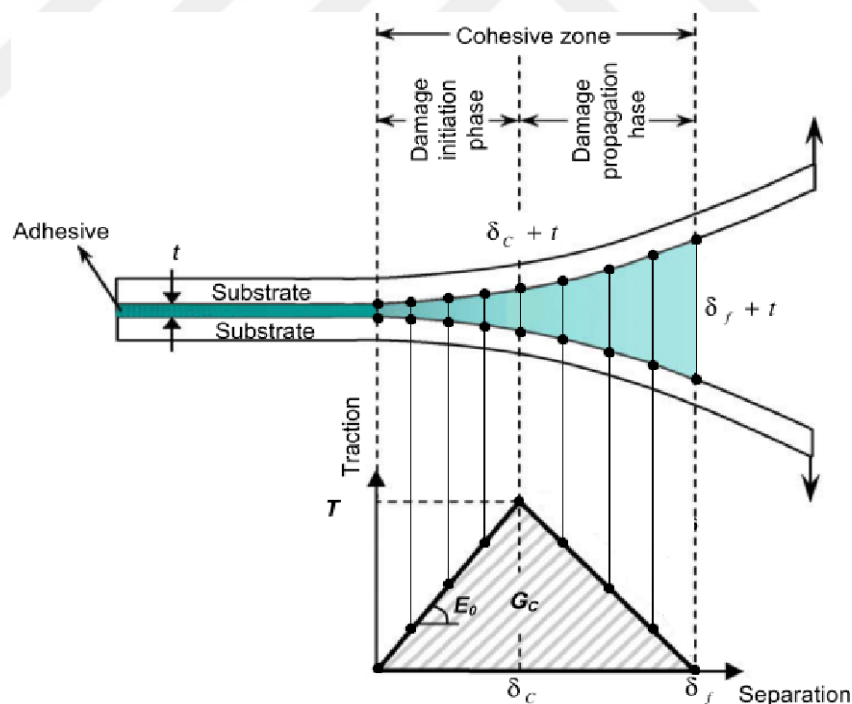
Figure 2.10 CZM crack propagation illustration (Noorman, 2014).

To obtain the most accurate results in this thesis, CZM properties for contact debonding is defined as the figure that is shown in Figure 2.11.

Properties of Outline Row 3: czm		
	A	B	
1	Property	Value	
2	⊟ 🔀 Fracture-Energies based Debonding		
3	Debonding Interface Mode	Mode I ▼	
4	Tangential Slip Under Normal Compression	No	
5	Maximum Normal Contact Stress	1E+05	Pa
6	Critical Fracture Energy for Normal Separation	0,25	J m^-2
7	Maximum Equivalent Tangential Contact Stress		Pa
8	Critical Fracture Energy for Tangential Slip		J m^-2
9	Artificial Damping Coefficient	0,001	s

Figure 2.11 CZM Properties (ANSYS V19)

As shown in the figure above, maximum normal contact stress is determined as 0.1 MPa from the recent studies (Irschick et all, 1996).

3. MATERIAL AND METHOD

In this thesis, there are two stages of the proposed method. These are;

1. Determination of constructional and controlled parameters of polymeric cylindrical beams,

2. Adhesion and friction force simulations of cylindrical beams,

3.1. Determination of Parameters of Polymeric Cylindrical Beams

Euler-Bernoulli beam theory with continuous contact and fracture mechanics is used for determination of constructional parameters. Adhesion characteristics and equivalent stiffness values with equivalent modulus of elasticity of cylindrical beams are obtained by using these theories and upper and lower values of respective force quantities are determined in constructional and controlled parameters. Parameters of beams are explained below.

- Constructional parameters: Beam diameter(D), height of beam(H), bore diameter(d) and bore height(h) within beam, modulus of elasticity(E) of beam.

- Controlled parameters: Pre-loading force, loading and unloading velocity, sliding velocity and pressure value of cavity within beam.

3.1.1. Constructional Parameters

Constructional parameters are directly related to dimensions of material. Beam diameter(D), height of the beam(H), bore diameter(d) and bore height of the beam(h) are constructional parameters those are directly related to design of the part.
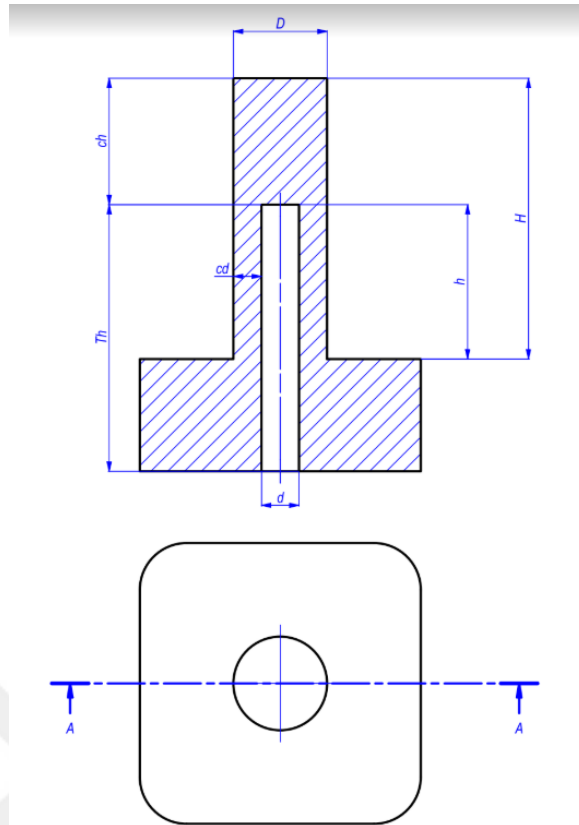
Figure 3.1 A section from technical drawing of PDMS pillar with defined dimensional parameters.

According the technical drawing that is shown in Figure 3.1, determined constructional parameters are shown in Table 3.1.

Table 3.1 Constructional parameters of the cylindrical beam

D	Outer Diameter
d	Bore Diameter
H	Height of the Beam
h	Bore Height
d*	d/D
h*	h/H

Modulus of elasticity(E) is structural parameter which is connected to material. In this thesis, PDMS has been chosen as the material of the cylindrical beams. Material properties of PDMS and flat glass plane are shown in the Table 3.2.

Table 3.2 Material Properties of PDMS cylindrical beam and flat glass plane

Material	PDMS Cylindrical Beam	Flat Glass Plane
Mass density	0.97 kg/m3	2500 kg/m3
Young's modulus	2.3 MPa	70 GPa
Poisson ratio	0.5	0.28

3.1.2. Setup of the Simulations

As it is mentioned in the thesis before, simulations have been set in the ANSYS finite element analysis program at the static structural module. The drawn parts to be used in the simulations and the direction of the motion are shown in the figure below.
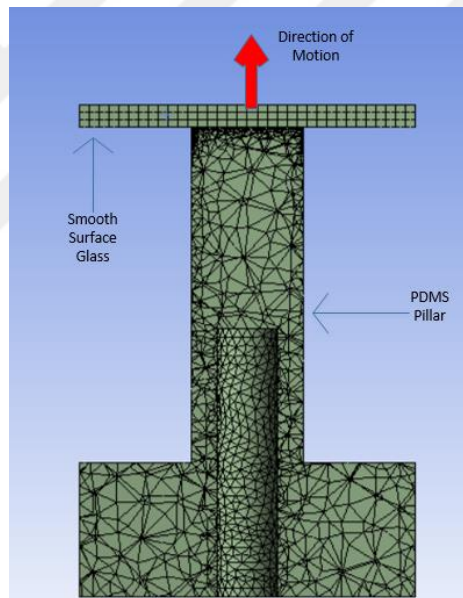
Figure 3.2 Illustration from the simulation setup with bored dimensional cylindrical beam and smooth glass part

3.1.3. Controlled Parameters of the Simulations

Loading and unloading velocity: These parameters are used in adhesion simulations. The effect of these parameters is not observed at these simulations. Loading and unloading velocity have been determined as 1 mm/sec at Z direction

Sliding velocity: This parameter is used in friction simulations. It has been determined as 2 mm/sec

Bore pressure of the beam: To observe pressure effect on the adhesion force, bore dimension of the beam is pressurized and these simulations are done by values between -0.5 MPa and 0.5 MPa.
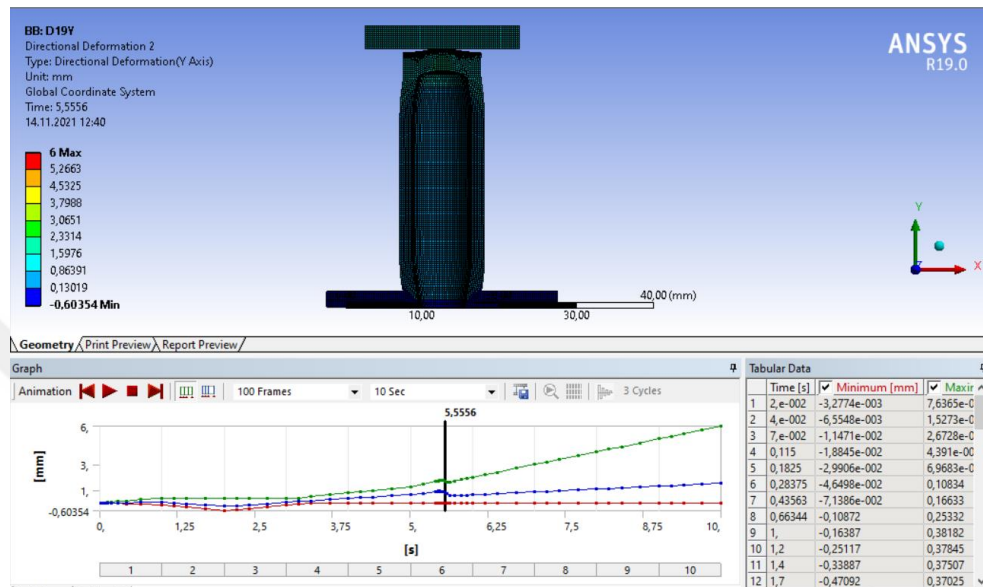
Figure 3.3 Sample simulation of cylindrical beam with pressurized bore dimension

3.2. Adhesion and Friction Simulations of the Cylindrical Beams with Bore Dimension

Simulation of cylindrical beam inlet pressurizing process is realized by fluent module in ANSYS program. Obtained results from Fluent module is used in structural analysis at the same program. This method is called One Way Fluid-Solid Interaction (FSI). If fluent and structural module in ANSYS is used simultaneously, it is called as Two-Way FSI.

In this thesis it is used One Way FSI method for analysing the effect of bore pressure. The figures shown below are captured from ANSYS program fluent module.
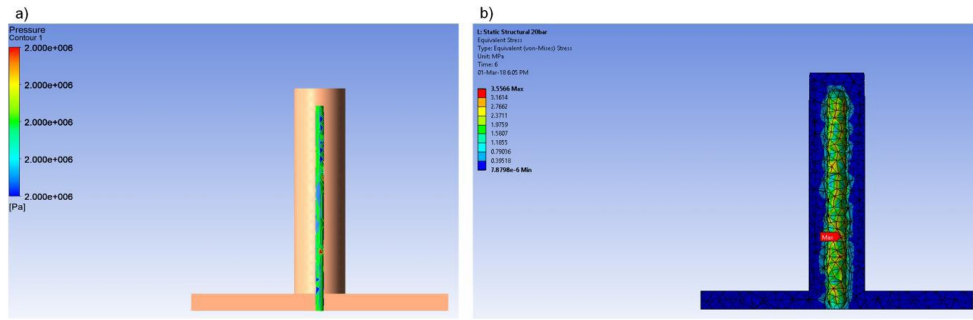
Figure 3.4 With One Way FSI method a) Pressure value from Fluent module, b) Stress and deformation results at structural analysis by using pressure value from Fluent module.

3.2.1. Adhesion simulations of the cylindrical beams with bore dimension

Simulations have been done by using finite element based engineering program. It is formed pre-loaded contact by given 0,5 mm displacement at –y direction. In this study, support layer is 2 mm thickness. Debonding contact stress have been determined as 0.1 MPa that has been cited CZM theory at the simulations (Aksak et all.).
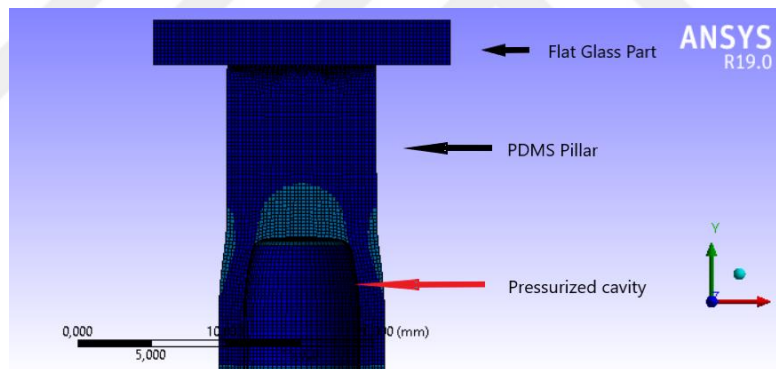
Figure 3.5 An illustration of simulations for the effect of pressurized cavity

Technical specifications of the cylindrical beam and smooth glass plane are given in Table 3.3.

Table 3.3 Material Properties of used solids

	PDMS	Glass Plane
Young Modulus	2.3 Mpa	70 GPa
Poisson Ratio	0.49	0.28
Density	970 kg/m³	2500 kg/m³

Determined dimensions of the beam and pressure that has been used for simulations are shown below in the tables.

Table 3.4 Determined parameters of the simulations

Outer diameter of the cylindrical beam	D	5, 10, 15mm
Height of the cylindrical beam	H	20, 30, 40 mm
Inner diameter of beam (bore diameter)	d	3, 6, 9 mm
Bore height of the beam	h	9, 18, 27 mm
Bore pressure	P	-0.5,-0.3,-0.1,0.1, 0.3, 0.5 MPa

Simulations have been determined according to parameters. Diameter effect, height effect and initially pressurized bore dimension effect on the adhesion have been examined. These simulations have been planned according to parameters which are shown in Table 3.5.

Table 3.5 Constructional and controlled parameters of adhesion simulations

	# of Simulation	D	d	Dia Ratio(d/D)	h	H	Height Ratio(h/H)	P/E	P(Mpa)
Outer Diameter Effect	D1	5	0	0	0	30	0	0	0
	D2	10	0	0	0	30	0	0	0
	D3	15	0	0	0	30	0	0	0
Outer Height Effect	D4	10	0	0	0	20	0	0	0
	D2	10	0	0	0	30	0	0	0
	D5	10	0	0	0	40	0	0	0
Inner Diameter and Height Effect	D2	10	0	0	0	30	0	0	0
	D6	10	3	0,3	9	30	0,3	0	0
	D7	10	6	0,6	9	30	0,3	0	0
	D8	10	9	0,9	9	30	0,3	0	0
	D9	10	3	0,3	18	30	0,6	0	0
	D10	10	6	0,6	18	30	0,6	0	0
	D11	10	9	0,9	18	30	0,6	0	0
	D12	10	3	0,3	27	30	0,9	0	0
	D13	10	6	0,6	27	30	0,9	0	0
	D14	10	9	0,9	27	30	0,9	0	0
Initially Pressurized Effect	D10	10	6	0,6	18	30	0,6	0	0
	D15	10	6	0,6	18	30	0,6	1	0,1
	D16	10	6	0,6	18	30	0,6	3	0,3
	D17	10	6	0,6	18	30	0,6	5	0,5
	D18	10	6	0,6	27	30	0,9	1	0,1
	D19	10	6	0,6	27	30	0,9	3	0,3
	D20	10	6	0,6	27	30	0,9	5	0,5
	D21	10	9	0,9	27	30	0,9	1	0,1
	D22	10	9	0,9	27	30	0,9	3	0,3
	D23	10	9	0,9	27	30	0,9	5	0,5
	D24	10	6	0,6	18	30	0,6	-1	-0,1
	D25	10	6	0,6	18	30	0,6	-3	-0,3
	D26	10	6	0,6	18	30	0,6	-5	-0,5
	D27	10	6	0,6	27	30	0,9	-1	-0,1
	D28	10	6	0,6	27	30	0,9	-3	-0,3
	D29	10	6	0,6	27	30	0,9	-5	-0,5

3.2.2. Friction simulations of the cylindrical beam with bore dimension

In the friction simulations, parameters were defined same as for adhesion simulations. Difference from adhesion simulations, glass part is moved -0.5 mm on the y-axis, then it is moved on the x-axis for observing the frictional force between glass and cylindrical part. Friction coefficient (μ) has been set 0.3 for these simulations. μ value has not been calculated for these simulations, because this value is kept constant all these simulations.

These simulations have been planned according to parameters which are shown in Table 3.6.

Table 3.6 Constructional and controlled parameters of friction simulations

	# of Simulation	D(mm)	d(mm)	Dia Ratio(d/D)	h(mm)	H(mm)	Height Ratio(h/H)	P/E	P(Mpa)
Outer Diameter Effect	D1F	5	0	0	0	30	0	0	0
	D2F	10	0	0	0	30	0	0	0
	D3F	15	0	0	0	30	0	0	0
Outer Height Effect	D4F	10	0	0	0	20	0	0	0
	D2F	10	0	0	0	30	0	0	0
	D5F	10	0	0	0	40	0	0	0
Inner Diameter and Height Effect	D2F	10	0	0	0	30	0	0	0
	D6F	10	3	0,3	9	30	0,3	0	0
	D7F	10	6	0,6	9	30	0,3	0	0
	D8F	10	9	0,9	9	30	0,3	0	0
	D9F	10	3	0,3	18	30	0,6	0	0
	D10F	10	6	0,6	18	30	0,6	0	0
	D11F	10	9	0,9	18	30	0,6	0	0
	D12F	10	3	0,3	27	30	0,9	0	0
	D13F	10	6	0,6	27	30	0,9	0	0
	D14F	10	9	0,9	27	30	0,9	0	0
Initially Pressurized Effect	D10F	10	6	0,6	18	30	0,6	0	0
	D15F	10	6	0,6	18	30	0,6	1	0,1
	D16F	10	6	0,6	18	30	0,6	3	0,3
	D17F	10	6	0,6	18	30	0,6	5	0,5
	D30F	10	9	0,9	18	30	0,6	1	0,1
	D31F	10	9	0,9	18	30	0,6	3	0,3
	D32F	10	9	0,9	18	30	0,6	5	0,5
	D18F	10	6	0,6	27	30	0,9	1	0,1
	D19F	10	6	0,6	27	30	0,9	3	0,3
	D20F	10	6	0,6	27	30	0,9	5	0,5
	D21F	10	9	0,9	27	30	0,9	1	0,1
	D22F	10	9	0,9	27	30	0,9	3	0,3
	D23F	10	9	0,9	27	30	0,9	5	0,5
	D24F	10	6	0,6	18	30	0,6	-1	-0,1
	D25F	10	6	0,6	18	30	0,6	-3	-0,3
	D26F	10	6	0,6	18	30	0,6	-5	-0,5
	D27F	10	6	0,6	27	30	0,9	-1	-0,1
	D28F	10	6	0,6	27	30	0,9	-3	-0,3
	D29F	10	6	0,6	27	30	0,9	-5	-0,5

3.3. Validation of the results in ANSYS Static Structural module from ANSYS Fluent module

Although the pressure can be applied to the part at static structural module in ANSYS finite element-based program, for validation of the static module pressure value has been applied at fluent module in ANSYS and obtained result has been transferred to the static structural module. Thus, the results obtained by establishing the One Way FSI system has been compared with the results obtained from static structural module. Stress distribution in the soft beam is shown in Figure 3.6 by different modules which are tatic Structural module and One Way FSI system.
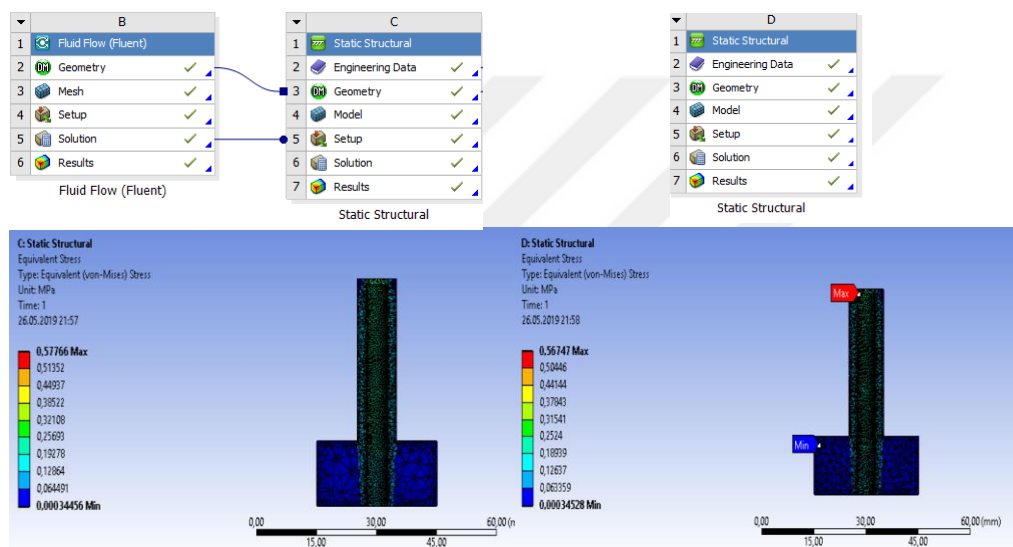
Figure 3.6 Stress and deformation results from a) One way FSI module, b) Static structural model of ANSYS

Based on this comparison, it has been decided to use ANSYS Static Structural module to run the simulations. Static structural module faster than One Way FSI. This gave the opportunity to run more simulations in less time and to increase the number of simulations.

4. RESULTS

4.1. Effect of Constructional and Controlled Parameters on Adhesion Force

As it is explained Table 3.3, simulations have been categorized by 3 different effects. Results have been examined by these effects separately. These effects are;

- Effect of outer diameter(D) and bore diameter(d): All parameters except for bore diameter(d) and outer diameter are kept constant. Force and displacement results are observed according to bore diameter(d) and outer diameter(D) variable.

- Height(H) and bore height(h) effect: All parameters except for bore height(h) and outer height(H) are kept constant. Force and displacement results are observed according to h and H variable.

- Initially pressurized bore effect: At these simulations, pressurized bore effect has been examined. The variation of the pressure change according to the bore diameter and bore height is observed by changing the pressure(P), bore height(h) and bore diameter(d) respectively.

4.1.1. Effect of outer and bore diameter on adhesion force

Simulations have been run by changing the bore diameter(d) and outer diameter(D). The adhesive force change and maximum displacement of beam tip are observed displacement and force results is shown in the table below.

Table 4.1 Adhesive force and displacement results of the beam by different outer diameter and bore diameter.

# of Simulation	D (mm)	d (mm)	Dia Ratio (d/D)	h (mm)	H (mm)	Height Ratio (h/H)	Fadh (N)	Elongation (mm)
D1	5	0	0	0	30	0	0,9281	0,6166
D2	10	0	0	0	30	0	2,9847	0,56295
D3	15	0	0	0	30	0	5,9638	0,47328
D6	10	3	0,3	9	30	0,3	3,0181	0,5804
D7	10	6	0,6	9	30	0,3	2,9835	0,62574
D8	10	9	0,9	9	30	0,3	3,0386	1,2476
D9	10	3	0,3	18	30	0,6	3,5981	0,66859
D10	10	6	0,6	18	30	0,6	3,1665	0,73914
D11	10	9	0,9	18	30	0,6	3,1015	1,8835
D12	10	3	0,3	27	30	0,9	3,2113	0,64792
D13	10	6	0,6	27	30	0,9	2,4871	0,69716
D14	10	9	0,9	27	30	0,9	2,0656	1,7057
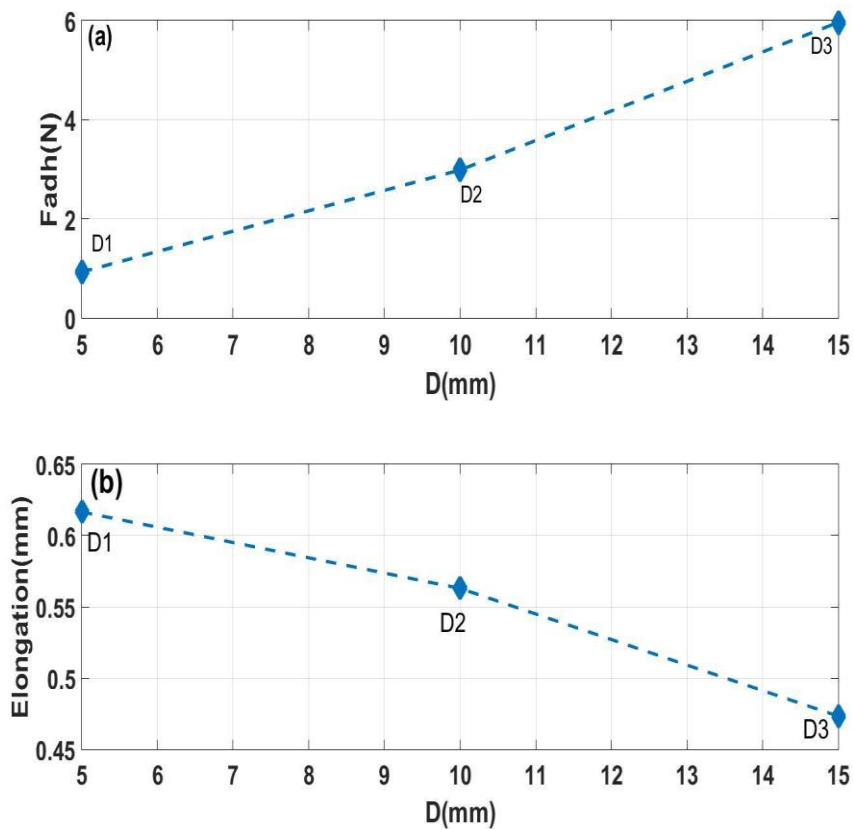
Figure 4.1 a) Adhesive force-outer diameter(D) b) Elongation-outer diameter(D) graphs of specimens

As it is shown the graphs in Figure 4.1, while outer diameter increases, adhesive force is increasing. For this reason, adhesive force is directly related to contact surface area. Opposite of the adhesive force, elongation will be decreasing because of the increase in rigidity of the part.

After the observing the outer diameter effect of the part, simulations run by observing bore diameter effect. The result graphs of these specimens are shown in the graphs below.
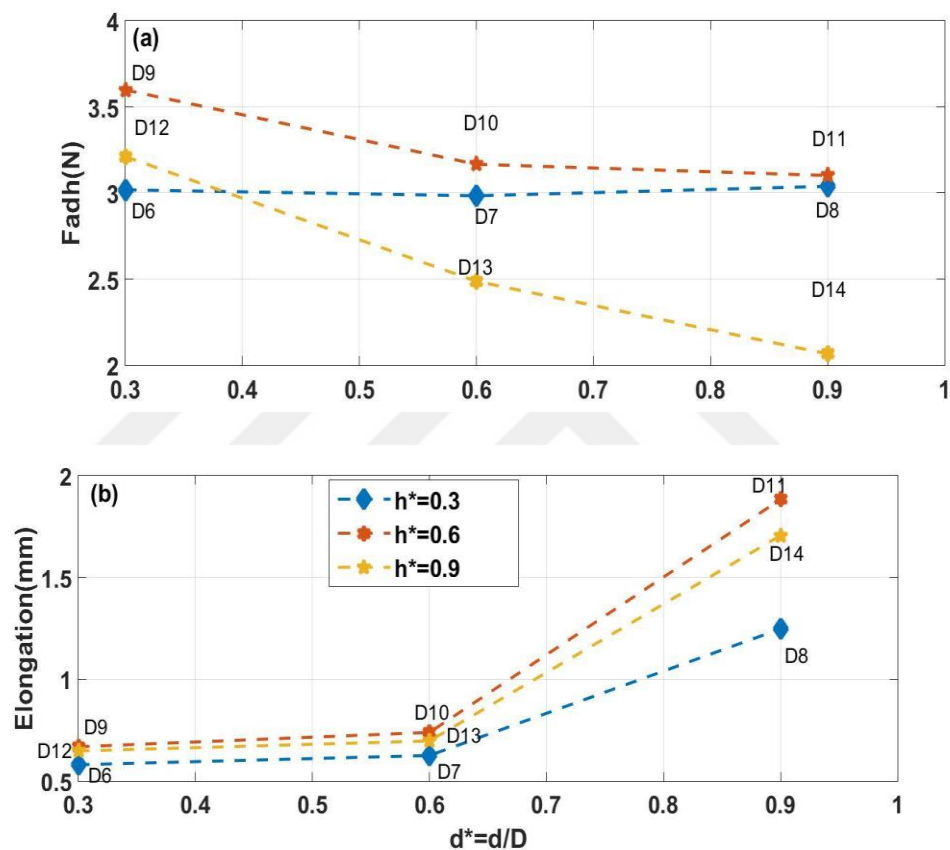
Figure 4.2 a) Adhesive force-bore diameter(D) b) Elongation-bore diameter(D) graphs of specimens

After outer diameter change results observed, outer diameter is chosen as 10 mm and bore diameter change results have been observed. At this part, simulation results have been observed by different bore height parameters which are 0.3, 0.6 and 0.9. When the graphs have been examined, change of bore diameter affect the adhesive force but effect of bore height on the adhesive force is more influential for tuning the adhesive force. Because, the biggest change of the adhesive force has been set in h*= 0.9 simulations.

4.1.2. Effect of height and bore height on the adhesion force

Simulations were made by changing outer height(H) and bore height(h). Bore diameter and outer diameter have been kept constant. The values of the parameters and results of adhesive force and displacement values are shown in table below.

Table 4.2 Adhesion force and displacement results by different height and bore height.

# of Simulation	D (mm)	Dia Ratio (d/D)	H (mm)	Height Ratio (h/H)	Fadh (N)	Elongation(mm)
D4	10	0	20	0	3,0672	0,35296
D2	10	0	30	0	2,9847	0,56295
D5	10	0	40	0	2,8803	0,65148
D2	10	0	30	0	2,9847	0,56295
D6	10	0,3	30	0,3	3,0176	0,5804
D7	10	0,6	30	0,3	2,9835	0,62574
D8	10	0,9	30	0,3	3,0386	1,2476
D9	10	0,3	30	0,6	3,5981	0,66859
D10	10	0,6	30	0,6	3,1665	0,73914
D11	10	0,9	30	0,6	3,1015	1,8835
D12	10	0,3	30	0,9	3,2113	0,64792
D13	10	0,6	30	0,9	2,4871	0,69716
D14	10	0,9	30	0,9	2,0656	1,7057
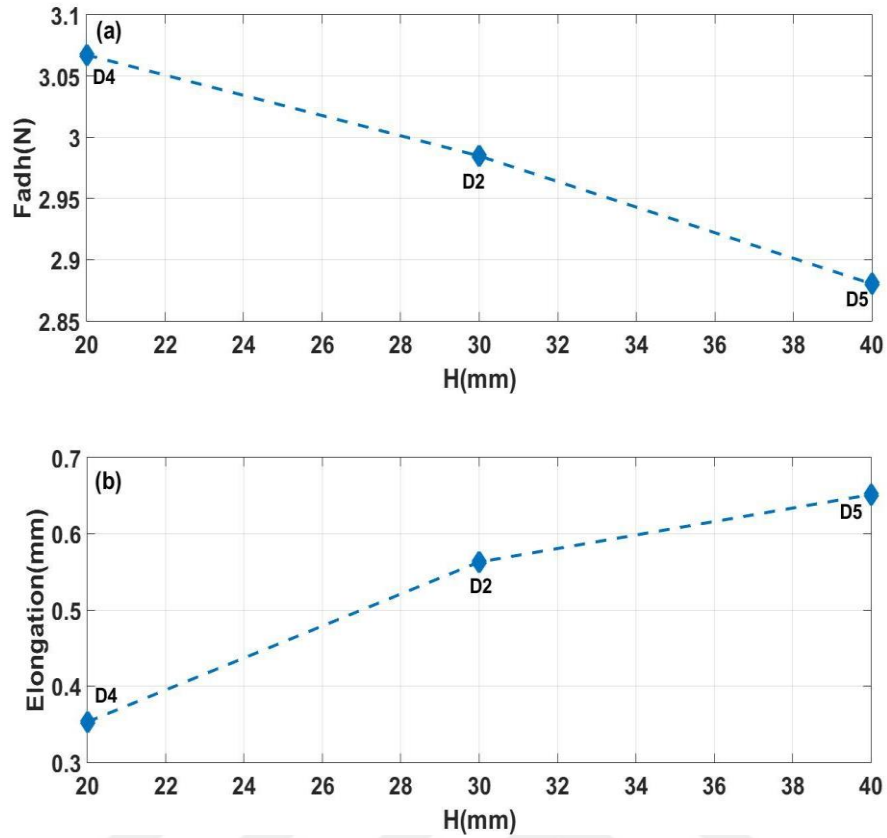
Figure 4.3 a) Adhesive force-height(H) b) Elongation-height graphs of specimens

Before observing the effect of bore height, effect of outer height of the pillar has been examined and graphs have been observed. According to graphs, while outer height of the beam is increased, adhesive force is decreased. This is because the rigidity of the part changes with increasing the height of the cylindrical beam.
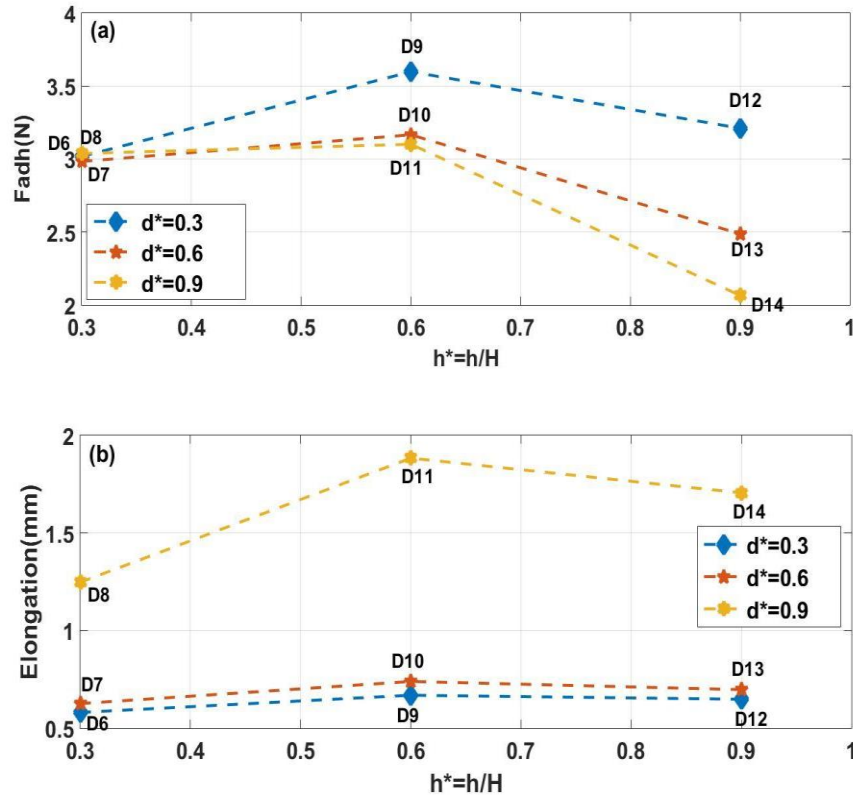
Figure 4.4 a) Adhesive force-bore height(H) b) Elongation-bore height graphs of specimens

When it is observed bore height effect, adhesive force first increases, then tends to decrease by all cavity diameter parameters. The reason of this, the rigidity of the cylindrical beam has been started to decrease when after h*=0.6 value.

4.1.3. Effect of bore pressure on adhesion force

At the next simulations, bore pressure has been altered as -0.5 and 0.5 MPa. According to the simulation results, adhesive force and displacement of the tip values are given in Table 4.3. As can be seen from the results, it is observed that adhesion force change is related to both applied pressure and change of constructional effects. At the same time, bore diameter did not cause much change in the adhesion force at different pressure values.

Table 4.3 Adhesion force and elongation results by different pressure values in the bore dimension.

# of Simulations	Dia Ratio (d/D)	Height Ratio (h/H)	P (Mpa)	Fadh (N)	Elongation (mm)
D10	0,6	0,6	0	3,1665	0,73914
D15	0,6	0,6	0,1	3,6338	0,8905
D16	0,6	0,6	0,3	4,5329	1,5002
D17	0,6	0,6	0,5	6,0885	2,093
D18	0,6	0,9	0,1	3,1173	0,9797
D19	0,6	0,9	0,3	2,746	1,7627
D20	0,6	0,9	0,5	0,6726	2,1169
D21	0,9	0,9	0,1	0,2232	2,4972
D22	0,9	0,9	0,3	0,4509	2,8546
D23	0,9	0,9	0,5	0,68503	4,6498
D24	0,6	0,6	-0,1	3,5606	0,6769
D25	0,6	0,6	-0,3	5,4703	0,6653
D26	0,6	0,6	-0,5	4,7503	0,4915
D27	0,6	0,9	-0,1	1,6944	0,6484
D28	0,6	0,9	-0,3	2,1983	0,3191
D29	0,6	0,9	-0,5	2,5662	0,2674

After constructional effects, simulations have been compiled same parameters with pressurized inlet. In order to observe the pressurized bore effect, samples with different design parameters have been simulated with different pressure values. According to graphs, pressure affect the adhesive force. But the adhesive force may be increase or decrease with pressure incrementation in the bore dimension. This is because the stress distribution at the contact point of the part is different at dissimilar constructional parameters.

To observe the effect of negative pressure on the adhesive force, simulations has been determined as shown in Table 4.3. According to these table, result graphs of these parameters are shown in figures below.
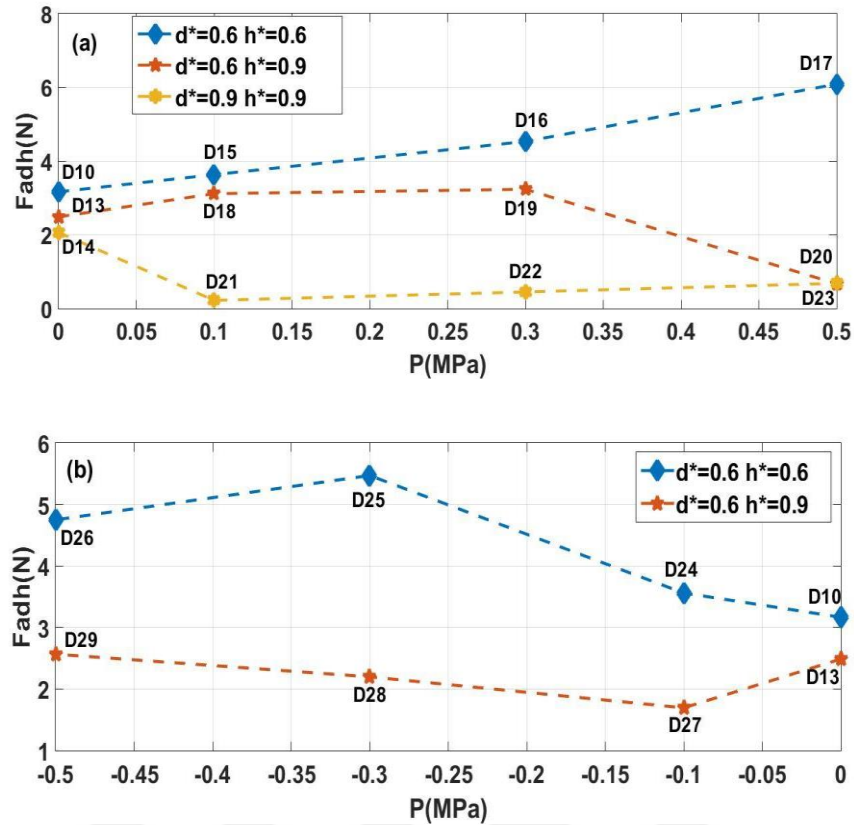
Figure 4.5 Adhesive force-pressure graph of the specimens a) Between 0 MPa and 0.5 MPa b) Between 0 MPa and -0.5 MPa

According to graphs above, pressure change in the gap of the cylindrical beam effect the adhesive force at the contact region. But, as can be seen very well in the graphs, pressure is not the only factor in increasing or decreasing the adhesive force. While the adhesive force increased at 0.6 diameter value, it showed a decreasing trend at 0.9 height value. This shows that the design parameters are also important for the desired adhesive force increase or decrease.

4.2. Effect of Constructional and Controlled Parameters on Friction Force

As in parts of adhesion, simulations separated according to 3 different effects. Results are examined by these effects separately. These effects are;

- Diameter effect: All parameters except for bore diameter(d) and outer diameter(D) are kept constant. Force and displacement results are observed according to d and D variable.

- Height effect: All parameters except for bore height(h) and beam height(H) are kept constant. Force and displacement results are observed according to h and H variable.

- Initially pressurized bore effect: At these simulations, pressurized bore effect has been examined. The variation of the pressure change according to the bore diameter and bore height is observed by changing the pressure(P), bore height(h) and bore diameter(d) respectively.

4.2.1. Effect of bore diameter and outer diameter on the friction force

Simulations were made by changing the bore diameter(d) and outer diameter(D). It is observed the frictional force change between these simulations.

Friction force results that have been obtained according to bore diameter(d) and outer diameter(D) are shown in Table 4.4.

Table 4.4 Frictional force values by different bore diameter and outer diameter.

# of Simulation	D (mm)	Dia Ratio (d/D)	H (mm)	Height Ratio (h/H)	Fk (N)
D1F	5	0	30	0	0,64051
D2F	10	0	30	0	0,77674
D3F	15	0	30	0	0,90161
D2F	10	0	30	0	0,77674
D6F	10	0,3	30	0,3	0,46893
D7F	10	0,6	30	0,3	0,34298
D8F	10	0,9	30	0,3	0,1165
D9F	10	0,3	30	0,6	0,3607
D10F	10	0,6	30	0,6	0,2416
D11F	10	0,9	30	0,6	0,0714
D12F	10	0,3	30	0,9	0,3279
D13F	10	0,6	30	0,9	0,18908
D14F	10	0,9	30	0,9	0,0521

As in adhesion simulations, an increase in outer diameter also increases the friction force. Because the surface area increases, the friction force also increases. The graph at the bottom side, bore diameter effect on the friction force is observed. When the bore diameter is increased, friction force is decreased inversely. The reason for this, bending stiffness of the cylindrical beam is decreased with bore diameter increase.
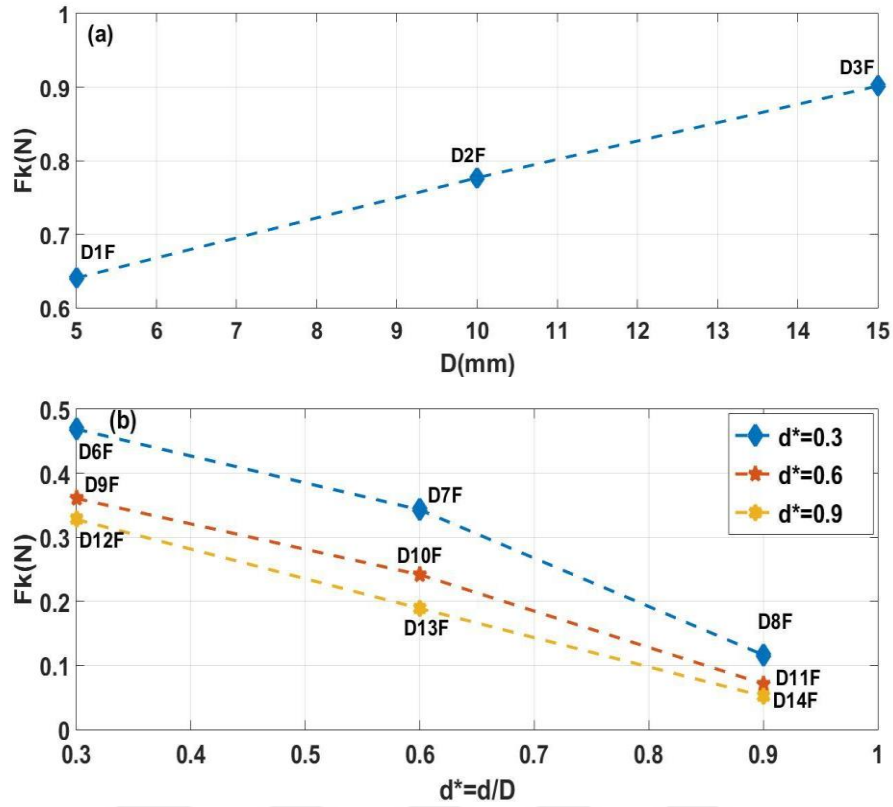
Figure 4.6 Force-diameter graphs of the specimens a) Fk-D b) Fk-d*

4.2.2. Effect of bore height and beam height on the friction force

Simulations were made by changing bore height(h) and beam height(H). Bore pressure(P) and bore diameter(d) have been stayed constant. Friction force results that have been obtained according to bore height and beam height are shown in Table 4.5.

Table 4.5 Frictional force values by different bore height and beam height.

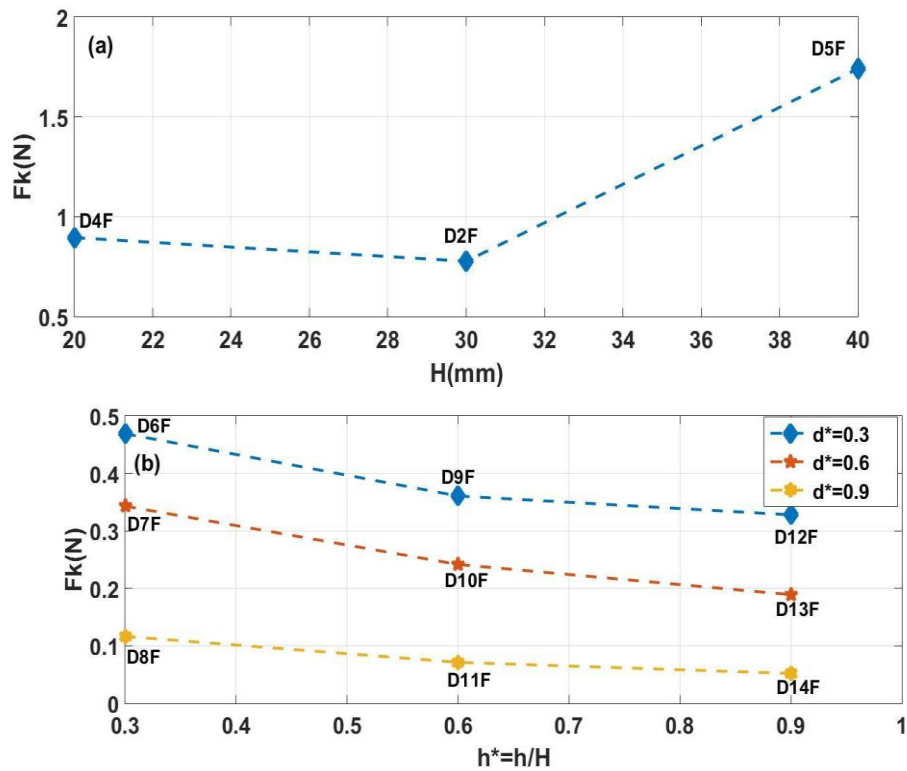| # of Simulation	D (mm)	Dia Ratio (d/D)	H (mm)	Height Ratio (h/H)	Fk (N)
D4F	10	0	20	0	0,8953
D2F	10	0	30	0	0,77674
D5F	10	0	40	0	1,7408
D6F	10	0,3	30	0,3	0,46893
D7F	10	0,6	30	0,3	0,34298
D8F	10	0,9	30	0,3	0,1165
D9F	10	0,3	30	0,6	0,3607
D10F	10	0,6	30	0,6	0,2416
D11F	10	0,9	30	0,6	0,0714
D12F	10	0,3	30	0,9	0,3279
D13F	10	0,6	30	0,9	0,18908
D14F	10	0,9	30	0,9	0,0521

Figure 4.7 Frictional force-height graphs of the specimens a) Fk-D b) Fk-d*

Unlike the diameter, height parameters effect the friction force differently. The friction force decrease at mid value of the beam height. The increment of friction force starts after the mid value of the beam height. The reason of this, when the height of the part

is increased, rigidity of the part is decreased. The same as bore diameter simulations, bore height increase affect inversely to friction force.

4.2.3. Effect of bore pressure on the friction force

As in adhesion simulations, bore pressure is altered between -0.5 MPa and 0.5 MPa in the frictional force simulations. According to simulation results, frictional force reaction has been observed.

To analyse and observe effect of negative pressure on the friction force, the simulations has been set at the pressure values between -0.5 MPa and -0.1 MPa.

The values of the parameters and results of frictional force values are shown in Table 4.6.

Table 4.6 Frictional force results of cylindrical beam by altered pressurized bore

# of Simulation	D (mm)	Dia Ratio (d/D)	H (mm)	Height Ratio (h/H)	P (Mpa)	Fk (N)
D10F	10	0,6	30	0,6	0	0,2416
D15F	10	0,6	30	0,6	0,1	0,9461
D16F	10	0,6	30	0,6	0,3	2,3627
D17F	10	0,6	30	0,6	0,5	3,7829
D30F	10	0,9	30	0,6	0,1	1,0848
D31F	10	0,9	30	0,6	0,3	3,1124
D32F	10	0,9	30	0,6	0,5	5,1402
D18F	10	0,6	30	0,9	0,1	1,2348
D19F	10	0,6	30	0,9	0,3	3,3184
D20F	10	0,6	30	0,9	0,5	5,4026
D21F	10	0,9	30	0,9	0,1	1,0194
D22F	10	0,9	30	0,9	0,3	2,9554
D23F	10	0,9	30	0,9	0,5	4,8917
D24F	10	0,6	30	0,6	-0,1	0,7091
D25F	10	0,6	30	0,6	-0,3	2,1328
D26F	10	0,6	30	0,6	-0,5	3,5581
D27F	10	0,6	30	0,9	-0,1	0,9431
D28F	10	0,6	30	0,9	-0,3	2,8389
D29F	10	0,6	30	0,9	-0,5	4,7355

As it expected from the simulations, absolute pressure increment in the bore dimension will be increase the friction force. Reason of this situation, pressure directly increase the bending stiffness of the part.
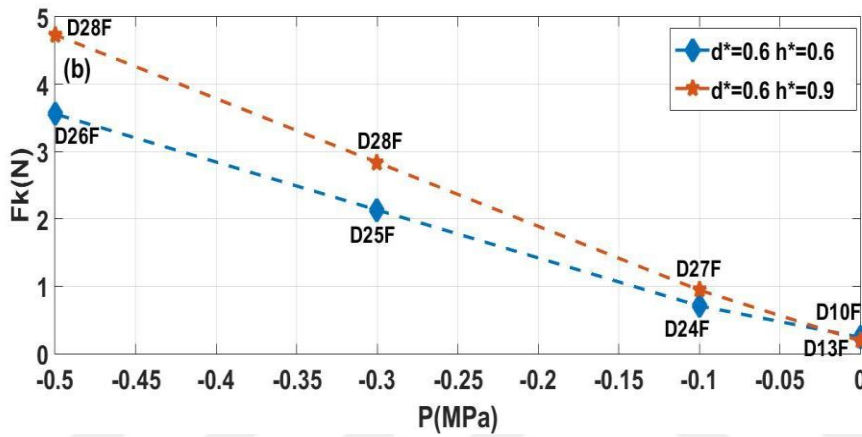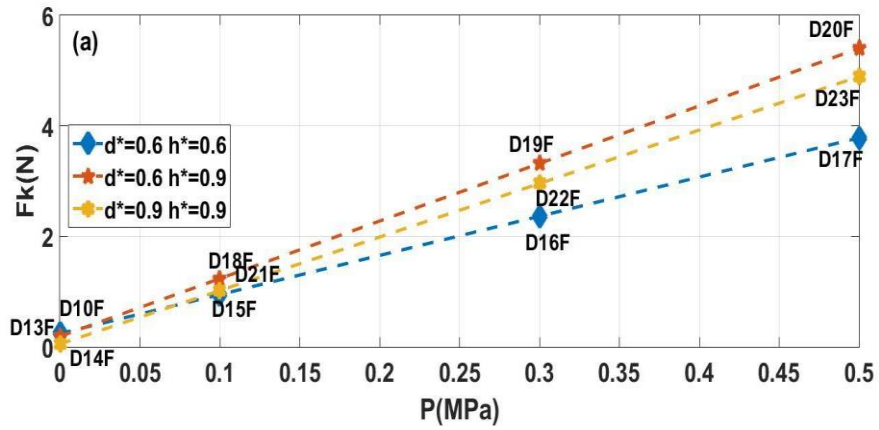
Figure 4.8 Friction force-pressure graph of the specimens a) Between 0 MPa and 0.5 MPa b) Between 0 MPa and -0.5 MPa

5. DISCUSSION

5.1. Discussion the effects of constructional and controlled parameters on the adhesion force of the cylindrical soft beam

In order to better observe the effect of the pressurized bore, it is necessary to observe the pressurized and unpressurized samples at the same design parameters. Comparison of pressured and unpressurized samples with the same bore diameter and height has been shown in Figure 5.1.
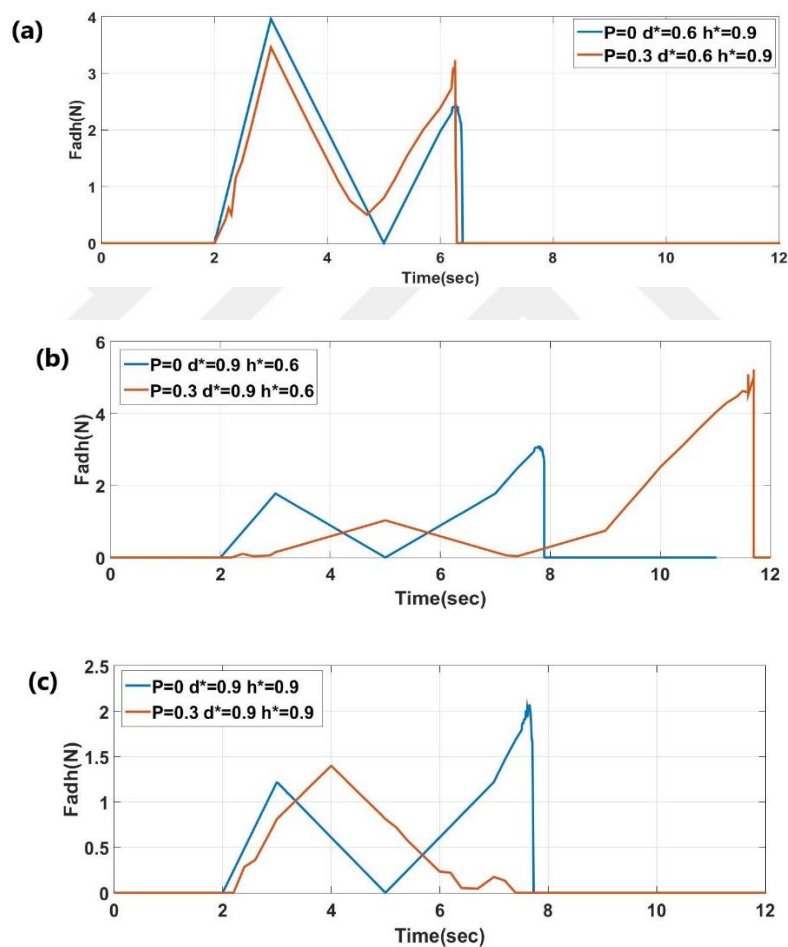

Figure 5.1 Adhesive force comparison between the effects **a)** d*=0.6 h*=0.9 **b)** d*=0.9 h*=0.6 **c)** d*=0.9 h*=0.9

As can be seen from the graphs, it has been observed that the adhesive force changes with the pressurized bore at the same constructional parameters at the time of separation.

Adhesive force can be controlled by pressure altering. However, if the adhesive force control is desired with pressure actuation, the constructional parameters are more important also. Because the force can be increased or decreased according to the selected design parameters.

Simulation results are shown that adhesion force can be altered by constructional or controlled effects. But pressure actuation is the one of the effective way for tuning the adhesive force in the soft beam.

Nevertheless, constructional parameters affect the adhesive force and elongation of the soft beam. Altering the bore height is more effective than altering the bore diameter.

Finally, constructional effects are not more desirable to control adhesive force because of low manufacturability of desired dimensions. If adhesive force control is desired, using the pressurized cavity will be more efficient and controllable. Adhesive force and elongation of the beam tip can be adjusted as desired with pressure actuation in the bore dimension. But the most important point to be considered is that the adhesive force control can be done with pressure, but it is necessary to choose the structural parameters according to the desired adhesive forces.

5.2. Discussion the effects of constructional and controlled parameters on the friction force of the cylindrical soft beam

Simulation results are shown that friction force can be altered by constructional or controlled parameters. As can be seen in the graphs below, it has been observed that the friction force can be changed significantly with pressure control at the same constructional parameters.

Pressurized and unpressurized comparison graphs of different constructional parameter samples are shown in the graphs below.
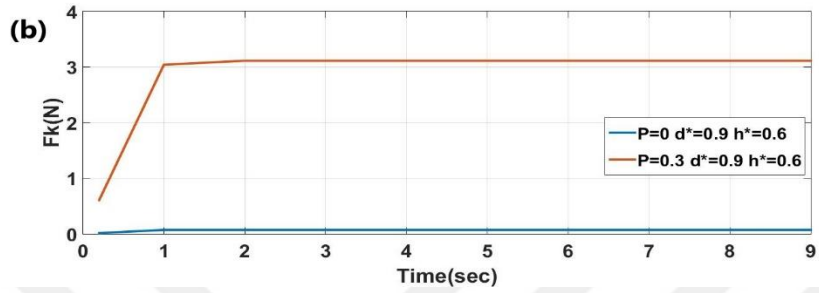
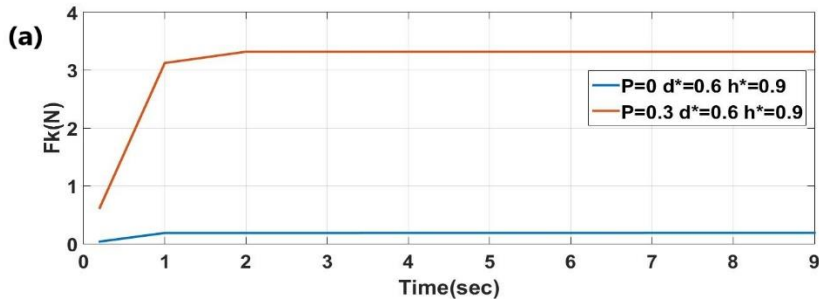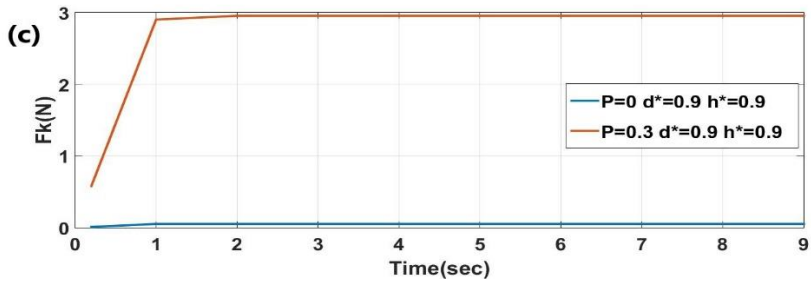Figure 5.2 Friction force comparison between the effects **a)** d*=0.6 h*=0.9 **b)** d*=0.9 h*=0.6 **c)** d*=0.9 h*=0.9

Simulation results are shown that friction force can be altered by constructional or controlled parameters. As can be seen in the graphs in Figure 5.2, it has been observed that the friction force can be changed significantly with pressure control at the same constructional parameters.

6. CONCLUSION AND RECOMMENDATIONS

In this thesis, contact forces of pneumatically actuated soft beams are numerically simulated. Simulations has been set for observing the desired effects. Adhesion force and maximum elongation of the contact point of the beam has been obtained these simulations.

It has been demonstrated that pneumatically driven of the soft cylindrical beam is one of the effective way for controlling the contact forces of the soft beams. These cylindrical beams can be tuned at desired contact force and elongation values by altering the pressure without any change of setting the construction parameters of the beam.

In this thesis, it has been proven that the pressure actuation method is one of the effective way to control both adhesion and friction force, but appropriate structural parameters should be used for this method to be more effective.

6.1. Future Work

In this thesis, adhesion and friction forces of the soft beam are numerically simulated and these forces tuned by altering the constructional and controlled parameters. To analyse and compare the simulation results experimentally, it has been prepared PDMS pillar specimens at different beam height, beam diameter and cavity of beam in further studies. In order to produce these samples in different sizes using a single mold, a complex mold design must be drawn. Assembly drawing of the die is shown in the figure below.
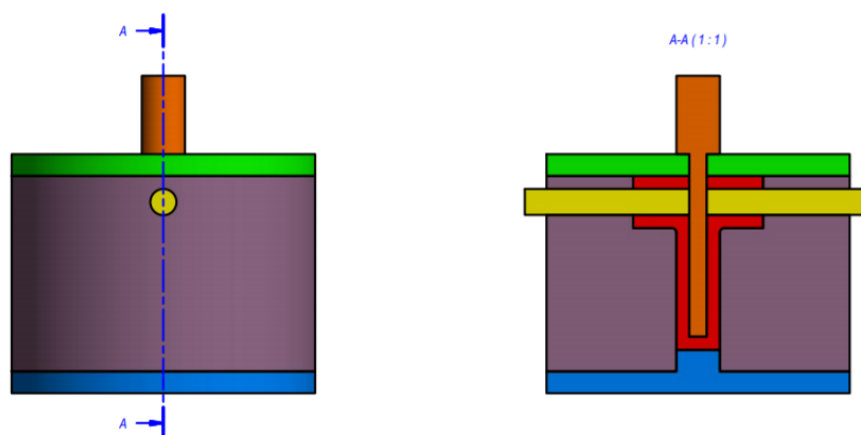

Figure 6.1 Assembly drawing of the molding

REFERENCES

Alfano, M., Furgiuele, F., Leonardi, A., Maletta, C., & Paulino, G. H. (2007). Cohesive Zone Modeling of Mode I Fracture in *Adhesive Bonded Joints. Key Engineering Materials, 348–349*, 13–16. https://doi.org/10.4028/www.scientific.net/kem.348-349.13

Arslan, A., Masjuki, H. H., Kalam, M. A., Varman, M., Mufti, R. A., Mosarof, M. H., ve Quazi, M. M. (2016). Surface texture manufacturing techniques and tribological effect of surface texturing on cutting tool performance: a review, *Critical Reviews in Solid State and Materials Sciences, 41*(6), 447-481.

Autumn, K., Gravish, N. (2008). Gecko adhesion: evolutionary nanotechnology. *Philosophical Transactions of the Royal Society of London A: Mathematical, Physical and Engineering Sciences*, *366*(1870), 1575-1590.

Barreau, V., Hensel, R., K. Guimard, N., Ghatak, A., M. McMeeking, R., Arzt, E. (2016). Fibrillar Elastomeric Micropatterns Create Tunable Adhesion Even to Rough Surfaces. *Advanced Functional Materials. 26.* 10.1002/adfm.201600652.

Brörmann, K., Barel, I., Urbakh, M. and Bennewitz, R. (2013). Friction on a microstructured elastomer surface. *Tribology Letters, 50*(1), 3-15.

Degrandi-Contraires, E., Poulard, C., Restagno, F., and Léger, L. (2012). Sliding friction at soft micropatterned elastomer interfaces. *Faraday discussions, 156*(1), 255-265.

Eray, T., Sümer, B., and Koc, I. M. (2016). Analytical and experimental analysis on frictional dynamics of a single elastomeric pillar, *Tribology International*, 100, 293-305.

Etsion, I., 2005. State of the art in laser surface texturing, *Journal of tribology, 127(1)*, 248-253.

Gao, J. P., Luedtke, W. D., Gourdon, D. Ruths, M., Israelachvili, J. N., Landman, U. (2004) Frictional forces and Amontons' law: *From the molecular to the macroscopic scale. J. Phys. Chem.*, *108*, 3410.

Hartlen, D. C., Montesano, J., & Cronin, D. S. (2020) Cohesive Zone Modeling of Adhesively Bonded Interfaces: The Effect of Adherend Geometry, Element Selection, and Loading Condition.

He, B., Chen, W., and Wang, Q. J. (2008). Surface texture effect on friction of a microtextured poly (dimethylsiloxane)(PDMS). *Tribology Letters, 31*(3), 187

Huang, W., Wang, X. (2013). Biomimetic design of elastomer surface pattern for friction control under wet conditions. *Bioinspiration & biomimetics, 8*(4), 046001.

Irschick, D. J.; Austin, C. C.; Petren, K.; Fisher, R. N.; Losos, J. B.; Ellers, O. *Biol. J. Linn. Soc.* **1996,** *59,* 21–35.

Kim, S., Aksak, B. and Sitti, M. (2007). Enhanced friction of elastomer microfiber adhesives with spatulate tips, *Applied Physics Letters, 91*(22), 221913

Kumar, A. A. Robotics [PowerPoint Slide]. Lecture Notes Online Web Site: https://www.iare.ac.in/sites/default/files/PPT/ROBOTICS-LATEST-PPT.pdf

Mao, B., Sidaiah, A., Liao, Y., Menezes, P. (2020). Laser surface texturing and related techniques for enhancing tribological performance of engineering materials. *A review, Journal of Manufacturing Processes*, *53*, 153-173, ISSN 1526-6125.

Marvi, H., Han, Y., and Sitti, M. (2015). Actively controlled fibrillar friction surfaces. *Applied Physics Letters, 106*(5), 051602.

Murarash, B., Itovich, Y., and Varenberg, M. (2011). Tuning elastomer friction by hexagonal surface patterning. *Soft Matter, 7*(12), 5553-5557.

Nasab, A.M., Luo, A., Sharifi, S., Turner, K.T., Shan, W. (**2020)** *ACS Applied Materials&Interfaces* 12 (24),27717-27725 DOI:10.1021/acsami.0c05367

Noorman, D.C. (2014). Cohesive Zone Modelling in Adhesively Bonded Joints: Analysis on crack propagation in adhesives and adherends.

Prieto-López, L. O., Williams, J. A. (2016). Using microfluidics to control soft adhesion, *Journal of Adhesion Science and Technology, 30:14*, 1555-1573, DOI:10.1080/01694243.2016.1155878

Varenberg, M., Gorb, S. (2007). Shearing of fibrillar adhesive microstructure: friction and shear-related changes in pull-off force. *Journal of The Royal Society Interface, 4*(15), 721-725.

Voyer, Joel, Ausserer, Florian, Klien, Stefan, Velkavrh, Igor, Diem, Alexander. (2017). Reduction of the Adhesive Friction of Elastomers through Laser Texturing of Injection Molds. Lubricants. 5. 45. 10.3390/lubricants5040045.

Yu, J., Chary, S., Das, S., Tamelier, J., Turner, K. L. and Israelachvili, J. N. (2012). Friction and Adhesion of Gecko-Inspired PDMS Flaps on Rough Surfaces: *Langmuir, 28*, 11527−11534, dx.doi.org/10.1021/la301783q

Zeng, H., Pesika, N., Tian, Y., Zhao, B., Chen, Y., Tirrell, M., and Israelachvili, J. N. (2009). Frictional adhesion of patterned surfaces and implications for gecko and biomimetic systems. *Langmuir, 25*(13), 7486-7495.

APPENDIX 1 (TECHNICAL DRAWING OF THE BEAM)
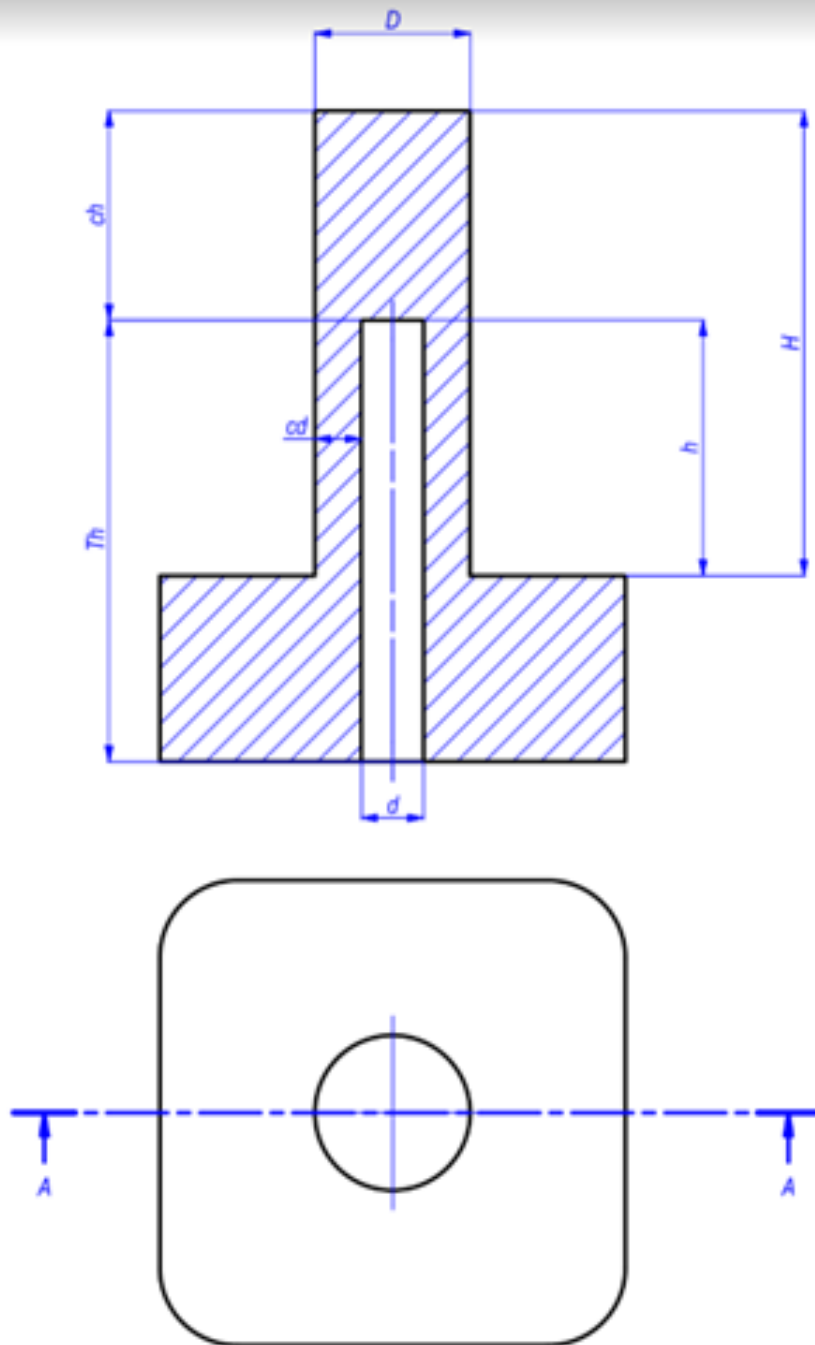
T.C.

AYDIN ADNAN MENDERES UNIVERSITY

GRADUATE SCHOOLOF NATURAL AND APPLIED SCIENCES

SCIENTIFIC ETHICAL STATEMENT

I hereby declare that I composed all the information in my master's thesis entitled EFFECT OF BORE DIMENSION AND PRESSURE ON THE CONTACT FORCES OF A SOFT BEAM within the framework of ethical behavior and academic rules, and that due references were provided and for all kinds of statements and information that do not belong to me in this study in accordance with the guide for writing the thesis. I declare that I accept all kinds of legal consequences when the opposite of what I have stated is revealed.

……………………..

Tuncay Burcay YILDIRIM

… / … / …